Title
Experimental Simulation of a Tangential Injection Swirl Flow Phase Separator for Desalination

Author
Jen, Jin

Publication Date
2023

Peer reviewed|Thesis/dissertation

UNIVERSITY OF CALIFORNIA

Los Angeles

Experimental Simulation of a Tangential Injection Swirl Flow Phase Separator for Desalination

A thesis submitted in partial satisfaction

of the requirements for the degree Master of Science

in Mechanical Engineering

by

Jin Jen

2023

ABSTRACT OF THESIS

Experimental Simulation of a Tangential Injection

Swirl Flow Phase Separator for Desalination

by

Jin Jen

Master of Science in Mechanical Engineering

University of California, Los Angeles, 2023

Professor Vijay K. Dhir, Chair

The experimental data of a simulation for a desalination system utilizing swirl flow phase separation is presented. Previously, the author investigated a desalination system that utilizes flash evaporation and swirl flow phase separation. To better understand the requirements for high separation efficiency, adiabatic experiments with air and water were conducted with a similar test section. In the experiments, air and water are premixed prior to entering the injection tubes and injection passages. The two-phase mixture tangentially injected into the test section experiences centrifugal force. Centrifugal force pushes heavier liquid toward the wall and air being lighter stays in the inner core. A retrieval tube that is placed in the center of the separator tube collects

the air from the air core. Superficial air and water velocities were parametrically varied. Air core diameter, air core coverage length, and separation efficiency were measured. It was found that air core coverage length is a significant factor in determining the efficacy of phase separation. The diameter of the injector and the position of the retrieval tube inlet were also determined to be important parameters in the system.

The thesis of Jin Jen is approved.

Adrienne Lavine

Jeffrey D. Eldredge

Vijay K. Dhir, Committee Chair

University of California, Los Angeles

2023

Table of Contents

List of Figures

List of Tables

1 Introduction

1.1 Problem Background

Freshwater scarcity has become one of the most pressing issues for human development. Population growth, economic development, pollution, and climate change has accelerated the depletion of the planet's freshwater resources. The need to produce freshwater from unconventional water sources has become imperative. Unconventional water sources such as seawater and brackish ground water typically have high salinities. The process of removing the salts to utilize these water sources is known as desalination. To address the issue of freshwater scarcity, there has been a growing effort to provide potable water by desalination. The size and number of desalination plants globally have been increasing over the past decade. In order to meet the current and future demand of freshwater, developing scalable, energy-efficient, and cost-effective desalination systems becomes a priority.

Energy usage and the cost of implementation are the primary factors that drive the cost of desalinated water. The size of the desalination plant, design and configuration of the desalination process contribute significantly to the cost of desalinated water. Therefore, implementing a desalination process that is compact and requires less land area could significantly reduce the cost.

In a recent study, the author investigated a novel system that combines both flash evaporation and phase separation through tangential injection. In this system, vapor production and phase separation occurred on the order of several milliseconds and phase separation efficiencies up to 99% were achieved [2]. With vapor production and phase separation occurring in a short amount of time and short distance, a compact system for desalination can be achieved which would reduce the costs associated with traditional thermal desalination methods. Parametric effects of liquid flowrate and available superheat were studied. Changes in vapor core length were observed to be significant on the efficiency of phase separation. Although qualitative observations were made, vapor core length and vapor core diameter in the separator tube necessary for high phase separation

efficiency was not thoroughly studied. This thesis investigates how core length and core diameter vary with inlet conditions as well as their influence on phase separation efficiency. Adiabatic experiments with air and water as the working fluids were conducted using the same test section. The effect of the position of the retrieval tube as well as the effect of injector diameter was also investigated.

1.2 Literature Review

With increasing scarcity of freshwater resources, desalination has emerged as a crucial technology to meet the growing demand for clean and potable water. According to a recent study, by 2030, the demand of water is expected to increase by 40% and more than 160% of the total available water volume in the world will be needed to satisfy the global water requirements [15]. There is an urgent need for developing desalination technologies that are economical and cost-effective. To tackle the issue of freshwater scarcity, there has been constant effort to produce potable water by desalination. As of the middle of February 2020, the global installed desalination capacity for freshwater production stood at 97 million cubic meters per day [5]. The size and number of of desalination plants have been on the increase at an average annual rate of about 6.8% since 2010. Two of the major desalination approaches are thermal-based systems and membrane-based systems.

Thermal-based desalination systems produce freshwater by evaporation of saline feed water and subsequent condensation. The most common and commercially implemented thermal desalination technologies are multistage flash evaporation (MSF) and multi-effect distillation (MED). These processes mainly differ by the operating temperature and pressure at which the saline feed water is boiled to produce vapor. For multistage flash evaporation, the once through (OT) configuration is expected to increase in number of plants. The MSF-OT process consists of two main sections which are the brine heater (heat input) and flashing stages (heat recovery). Initially, saline feed water flows through a set of heat exchanger tubes and is preheated prior to entering the the brine heater. The feed water is heated using thermal energy from low pressure bleed steam until it reaches

a temperature of 90 to 100 $^{\circ}C$ [11]. Heated saline water then enters the first stage where the ambient pressure is lower than the pressure in the brine heater. This decrease in pressure causes flashing of the saline water. The flashing vapor condenses on the heat exchanger tubes and loses latent heat to the saline feed water flowing inside the tubes. Distillate water is collected on a tray while the remaining saline water enters the next stage under lower pressure. The same process is repeated until the brine reaches the final stage where it is discharged. A significant factor that affects energy consumption in MSF is scaling or fouling. At high temperatures, different types of salts such as magnesium hydroxide, calcium carbonate, and non-alkaline scales form deposits [14]. Additional units in the desalination plant include pretreatment of the feed and intake seawater streams. Treatment of the intake seawater is limited to simple screening and filtration. However, treatment of the feed seawater is more extensive and includes deaeration and addition of antiscalant and foaming inhibitors [4].

MED is one of the oldest desalination technologies. Thermal requirements in MED are lower than MSF because MSF requires large amounts of high-temperature steam to boil water, whereas in MED water is boiled at a lower temperature as the pressure is lower than the atmospheric pressure [3]. MED consists mainly of a condenser and multiple effects. Initially, saline feed water enters the condenser tubes where it gets preheated. Then, feed water is fed to the multiple effects in equal proportions. In each effect, saline feed water is sprayed on the outer surface of the evaporator tubes. In the first effect, water sprayed on the evaporator tubes vaporizes as it absorbs heat. Vapor formed from the evaporation of feed water is used as an energy source for successive effects. Vapors from the last effect are used to preheat saline feed water and the vapor condenses to produce fresh water [9]. The number of effects determines the amount of fresh water produced in the process. However, it is limited by the minimum temperature difference between the consecutive effects and the total temperature range in the process [8]. The interest in MED desalination technology has been rapidly growing in countries close to the Arabian Sea and the Persian gulf [10]. In these regions, the abundance of solar energy allows for a coupling of MED with solar power plants.

Membrane-based systems use a semipermeable membrane to separate salts for producing freshwater. Recently, thermal desalination technologies have been getting replaced with membrane-based processes in many parts of the world. The most common membrane-based process used in desalination plants is Reverse Osmosis (RO). Reverse Osmosis accounts for over 68% of the online desalination capacity largely due to its energy efficient process [1]. In RO, osmotic pressure is overcome by pressurizing the saline feed water in order to separate water from the salt [13]. Despite the low energy use and low cost of water in RO compared to thermal desalination processes, the real cost and total energy consumption continue to challenge implementation. High pressure pumps are the major consumers of energy in a RO desalination process. Membrane compaction, degree of surface fouling, temperature, recovery, and aging are several factors that affect the applied pressure [18]. In order to reduce energy consumption and in return lower operating costs, increasing pump efficiency is critical.

The major desalination technologies such as MSF, MED, and RO have seen signficant cost reduction due to technological advancements in the past few decades. However, further advancements in these technologies are likely to be incremental and significant reduction in cost is not expected. Most of the current advancements focus on energy and cost efficiency through advanced materials, and on improving system components such as high pressure pumps and heat recovery devices [12]. The capital costs, which include land and construction costs, typically account for 30 to 50% of the total cost of desalination since they require relatively large land areas [19]. Implementing a process that is compact and requires less area could significantly reduce the cost of desalination.

Tangential injection has been used as a method for producing swirl flow. Guo and Dhir investigated single- and two-phase heat transfer in a vertical flow with tangential injection. Swirl flow was shown to enhance heat transfer compared to purely axial flows. With tangential injection, up to fourfold increase in average heat transfer coefficient was observed for single-phase flow [7]. In addition, the same authors observed that centrifugal force from swirl flows aids in separation of phases with different densities independent of gravity [6]. Valentekovich et al. [16] demonstrated phase separation based on swirl

flow produced by tangential injection for microgravity applications. Valentekovich and Dhir used tangential injection for phase separation under low gas to liquid volume ratios. They reported 0.999 volume-based dryness fraction for the separated gas [17].

2 Experiment

2.1 Project History

The apparatus used for desalination of sea water consisted of primary and secondary tanks made of stainless steel with a capacity of 50 gal each, a centrifugal pump, 2.66 cm ID and 12 m long stainless-steel pipeline, tape heaters, a flowmeter, test section, and a condenser. A single-stage system consisting of one separator tube and a two-stage system consisting of two separator tubes to further improve the separation efficiency were both studied. A schematic of the experiment loop for the single-stage system is shown in Figure 2.1. The

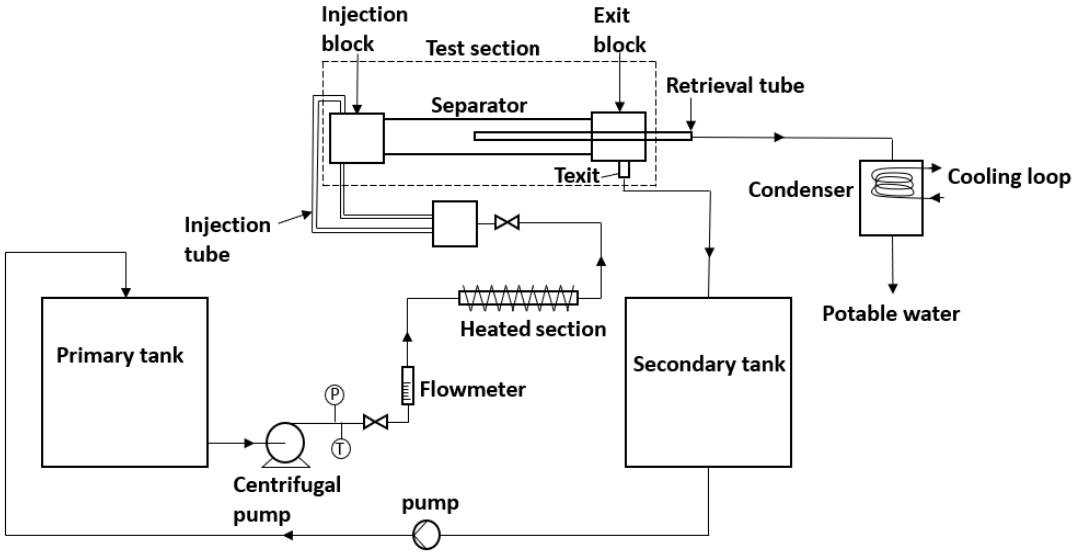

(a)

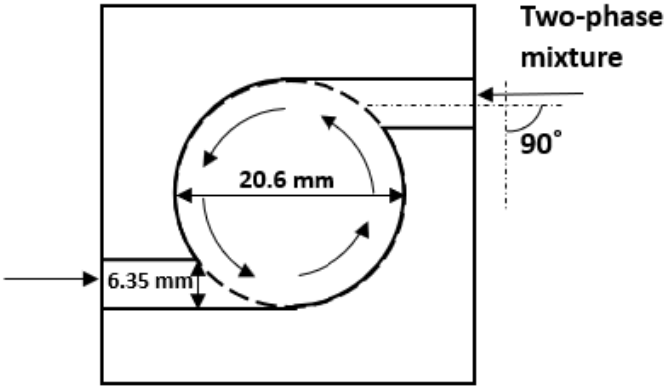

(b)

Figure 2.1: Setup used for single-stage dynamic flash evaporation and vapor separation system (a) experiment loop (b) injector configuration

test section consisted of an injection block made of aluminum, a 30.48 cm long and 2.06 cm ID borosilicate glass tube as the separator tube, an exit block made of aluminum through which a retrieval tube made of stainless steel is carried. The injection block had two injector passages that were each 6.35 mm ID and tangential to the separator tube. Two injection tubes which were each 30.48 cm long and 6.35 mm ID connect the water supply line to the injector passages in the injection block. The retrieval tube is mounted coaxially with the separator tube. In this system, subcooled pressurized feed water passes through injection tubes. As the heated water flows through the injection tubes, pressure drop occurs due to friction causing the initially subcooled liquid to be in a superheated state. The excess temperature drops as liquid flows through the tubes and flashing occurs to produce vapor. The two-phase mixture tangentially injected in the test section experiences centrifugal force. Centrifugal force pushes the heavier liquid toward the wall and vapor being lighter stays in the inner core. Vapor from the core is extracted using the retrieval tube placed at the center of the separator tube. The extracted vapor is directed to a condenser where condensation occurs at atmospheric pressure to produce potable water. The parametric effects of liquid flowrate and superheat on thermal conversion and phase separation efficiency were studied. The vapor core diameter and vapor core length were not measured.

2.2 Objective

In order to study core length, core diameter, and phase separation, adiabatic experiments with air and water were conducted. Air is similar in density to vapor and is significantly less dense than water. In the dynamic flash evaporation and vapor separation system, the vapor and water in the separator tube was at saturation temperature (around 100.5 $^{\circ}C$) and very close to atmospheric pressure (around 101.325 kPa). The density of vapor and water at these conditions are 0.60 kg/m^3 and 956 kg/m^3, respectively. In the adiabatic experiments, air and water are at room temperature (25 $^{\circ}C$) and close to atmospheric pressure in the separator tube. The density of air and water under these conditions are 1.16 kg/m^3 and 997 kg/m^3, respectively. In both experiments, the density of water is

much larger than the density of vapor and of air. As a result, an air core can be formed through tangential injection in the adiabatic experiments similar to that of the vapor core formed in the dynamic flash evaporation and vapor separation system. The experiments conducted were used to simulate the behavior of a vapor core in the separator tube as was observed in the previous experiments [2]. The goal of this study is to determine how the superficial velocities of water and air through the injection passages influence core length and core diameter and to investigate whether a minimal core length and core diameter is needed for high separation efficiency. To study the behavior of core length, core coverage length, which is the distance that the air core extends past the retrieval tube inlet, was measured rather than the total axial length of the air core. The experiments that have been performed include the measurement of air core diameter, air core coverage length and separation efficiency. The location of the retrieval tube position with respect to the length of the air core was viewed as an important parameter and was also studied.

2.3 Experimental Flow Loop

A single-stage configuration as used in the dynamic flash evaporation and vapor separation system was slightly modified and used. A schematic of the flow loop is shown in Figure 2.2.

An air supply line with a flowmeter was connected just before the injection tubes in order to mimic the two-phase liquid and vapor mixture inside the injection tubes and injection passages. The apparatus consisted of a primary tank made of stainless steel with a capacity of 50 gal, a centrifugal pump, 2.66 cm ID and 12 m long stainless-steel pipeline, a flowmeter, test section, and a collection tank. The test section consisted of an injection block made of aluminum, a 30.48 cm long and 2.22 cm ID acrylic tube as the separator tube, an exit block made of aluminum through which a retrieval tube made of stainless steel is carried. The injection block has two injector passages that are each 6.35 mm ID and tangential to the separator tube. The injector passage configuration is also shown in Figure 2.2. Two injection tubes which were each 30.48 cm long and 6.35 mm ID connect the water supply line to the injector passages in the injection block. The retrieval

tube is mounted coaxially with the separator tube. In these experiments, feed water is

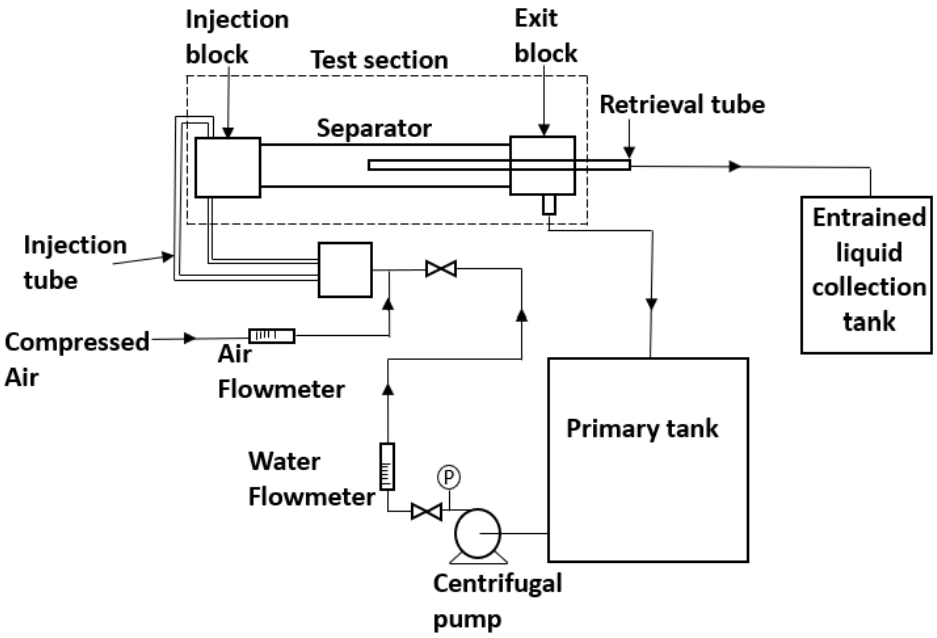

(a)

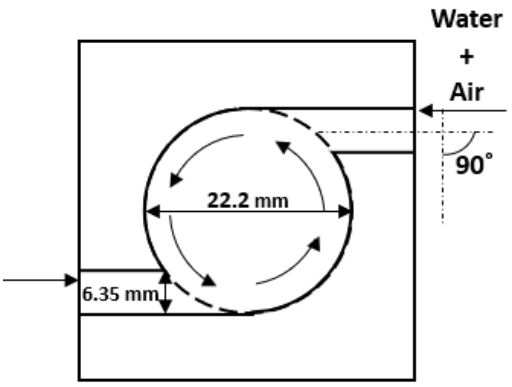

(b)

Figure 2.2: Setup used for adiabatic air and water experiments (a) experiment loop (b) injector configuration

stored in the primary tank at atmospheric pressure and maintained at room temperature. Water from the primary tank is pumped through the stainless-steel pipleine. Air from the air supply line is premixed with the water through a T connector. A two-phase mixture of air and water flows through the injection tubes and flows out of the injector passages which connect tangentially into the separator tube. The two-phase mixture tangentially injected in the test section experiences centrifugal force which pushes the heavier liquid toward the wall and allows for an air core to form. Air from the core is extracted using

the retrieval tube placed at the center of the separator tube and is directed to a collection tank at atmospheric pressure. The separated water is redirected from the exit block back to the primary tank.

2.4 Procedure

Air core diameter, air core coverage length, and phase separation efficiency were measured. A description of how these quantities were defined and measured will be presented in this section.

Core diameter (D_{core}) is the diameter of the air core defined by the air-water interfaces at the location of the retrieval tube inlet (see Figure 3.1 below). Similar to core length, a high-speed camera was used to take images and videos of the test section. The average core diameter was measured and recorded.

Core coverage length (L_{core}) is the axial length of the air core that extends beyond the inlet of the retrieval tube (see Figure 3.3 below). Core coverage length was measured from the location of the retrieval tube inlet to the location where the air core breaks apart and is no longer stable. This measurement was done by taking images and videos of the test section with a high-speed camera and measuring the distance from the retrieval tube inlet to the location where the air core breaks apart. In the experiments, the air core was observed to be fluctuating. Therefore, a maximum and minimum core coverage length for each case was measured and recorded.

Separation efficiency (η_s) represents how well the air is separated from the liquid as it is expected that there is a possibility of liquid from the annulus getting entrained into the air core. The separation efficiency is defined as the ratio of the injected mass flowrate of air to the total mass flowrate of air and the entrained liquid

$$\eta_s = \frac{\dot{m}_{air}}{\dot{m}_{air} + \dot{m}_{ent}} \tag{2.1}$$

where $\dot{m}_{air}$ represents the injected mass flowrate of air and $\dot{m}_{ent}$ represents the mass flowrate of water measured in the collection tank. Although some of air in the air core

gets carried with the liquid annulus, the amount of air is assumed to be small. It is assumed that all the air that is injected into the separator tube is collected through the retrieval tube.

In addition to measuring core diameter, core coverage length, and phase separation efficiency, the effect of retrieval tube position and the effect of injector diameter were studied. The effect of retrieval tube position was studied by varying the distance of the retrieval tube inlet to the injection passage and measuring the changes in core diameter, core coverage length and separation efficiency. Three different retrieval tube positions were studied. In addition, a larger injector diameter was also used to study the effect of tangential velocity of the liquid and air and its effect on core coverage length and separation efficiency.

The uncertainty (σ_R) in a quantity $R(x_1, x_2, ..., x_n)$ depending on variables $x_1, x_2, ..., x_n$ is calculated as

$$\frac{\sigma_R}{R} = \sqrt{\frac{1}{R^2}\left(\left(\frac{\partial R}{\partial x_1}\right)^2 \sigma_{x_1}^2 + \left(\frac{\partial R}{\partial x_2}\right)^2 \sigma_{x_2}^2 + ... + \left(\frac{\partial R}{\partial x_n}\right)^2 \sigma_{x_n}^2\right)} \tag{2.2}$$

where $\sigma_{x_1}, \sigma_{x_2}, ..., \sigma_{x_n}$ are the uncertainties associated with the measurement of each variable x. Using the above approach, the uncertainty in phase separation efficiency can be calculated as

$$\frac{\sigma_{\eta_s}}{\eta_s} = \sqrt{\left(\frac{\sigma_{\dot{m}_{air}}}{\dot{m}_{air}}\right)^2 + \left(\frac{\sigma_{(\dot{m}_{air}+\dot{m}_{ent})}}{(\dot{m}_{air}+\dot{m}_{ent})}\right)^2} \tag{2.3}$$

The uncertainty in $\dot{m}_{air}$ depends on the uncertainty in the air flowmeter. The uncertainty in $\dot{m}_{ent}$ depends on the mass of the liquid measured in the collection tank as well as the time measurements from a stopwatch. The measurement uncertainties are given in Table 2.1.

Table 2.1: Measurement Uncertainties

Parameter	Absolute Uncertainty
$\dot{V}_{water}$	0.2 GPM
$\dot{m}_{water}$	1.57×10^{-2} kg/s
$\dot{V}_{air}$	1 SCFM
$\dot{m}_{air}$	5.68×10^{-4} kg/s
D_{core}	0.34 mm
L_{core}	1.6 mm
η_s	3.2 - 12%

3 Results and Discussion

3.1 Core Diameter

In these experiments, water volume flowrate was varied from 1.5 GPM (95 cm^3/s) to 2.5 GPM (158 cm^3/s) and air volume flowrate was varied from 6 SCFM (0.17 m^3/min) to 10 SCFM (0.28 m^3/min). The superficial velocities of water and air in the injectors were varied. The superficial velocity of water (j_l) was defined as the volume flowrate of water divided by the total injector area as shown in Equation (3.1).

$$j_l = \frac{\dot{V}_{water}}{A_{inj,total}} \tag{3.1}$$

Similarly, the superficial velocity of air (j_g) was defined as the volume flowrate of air divided by the total injector area as shown in Equation (3.2).

$$j_g = \frac{\dot{V}_{air}}{A_{inj,total}} \tag{3.2}$$

For the given flowrates, j_l ranged from 1.6 m/s to 2.6 m/s and j_g ranged from 45 m/s to 75 m/s. The inlet of the retrieval tube was positioned 11.43 cm away from the injectors. The inner diameter and the outer diameter of the retrieval tube were 1.45 cm and 1.59 cm, respectively. The core diameter was measured from a set of images taken with a high speed camera. A photograph of the core diameter for liquid flowrate of 1.5 GPM and air flowrate of 10 SCFM is shown in Figure 3.1. As shown in the photograph, an air core diameter that is larger than the outer diameter of the retrieval tube is necessary to

prevent liquid from the annulus from entering into the retrieval tube.

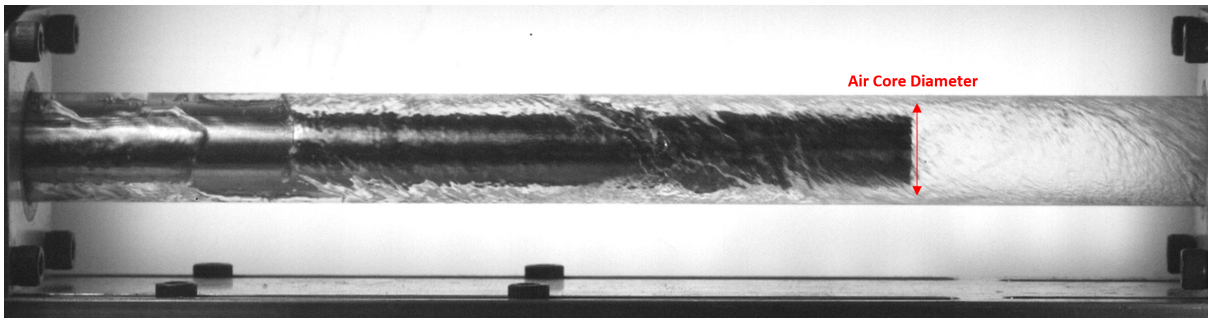

Figure 3.1: Photograph of Core Diameter for $\dot{V}_{water}$ = 1.5 GPM and $\dot{V}_{air}$ = 10 SCFM

For all cases investigated, the air core diameter is larger than the outer diameter of the retrieval tube and the air core fully envelopes the retrieval tube inlet as seen in the photograph. Figure 3.2 shows the behavior of air core diameter with changes in water and air flowrates. It is important to note that determining the air-water interfaces of

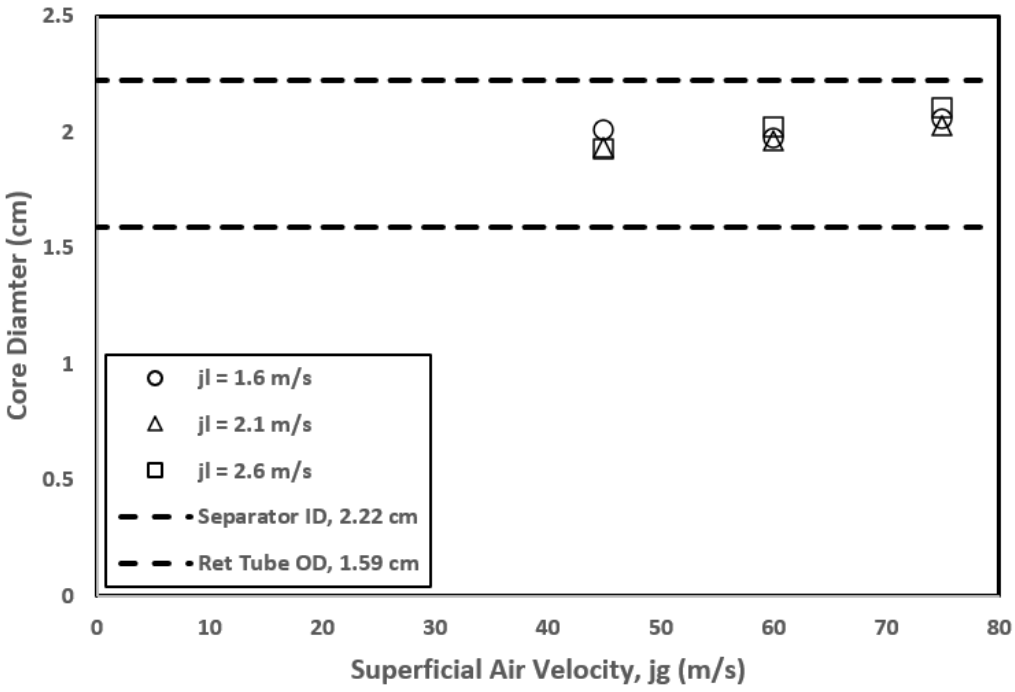

Figure 3.2: Air Core Diameter versus Superficial Air Velocity

the air core was very difficult due to the curvature of the separator tube. Although the uncertainty in the core diameter measurements were quite low as shown previously in Table 2.1, the exact location of the air-water interfaces was not well defined for each case. The air-water interfaces were determined from the author's observation and judgement of the images.

The changes in air core diameter are very small and all measurements are ±10 % of each other with respect to changes in air and water velocities. Air core diameter slightly increases with increase in air velocity at a given water velocity. This can be observed through the cases where liquid superficial velocity is 2.1 m/s and 2.6 m/s. This is intuitive considering the ratio of air momentum to liquid momentum is increasing. Therefore, higher air volume flowrate at a constant water volume flowrate increases the size of the air core. Higher tangential momentum leads to higher centrifugal force which creates a thicker and more stable air core. Air core diameter did not vary signficantly for the range of flowrates tested.

3.2 Core Coverage Length

The core coverage length was also measured for the previous experiments using the same camera images as used for measuring core diameter. The distance from the retrieval tube inlet to the location where the air core collapsed was measured. The inlet of the retrieval tube was positioned 11.43 cm away from the injectors. A photograph of the air core coverage length is shown in Figure 3.3. This is the same photograph as used in the previous section.

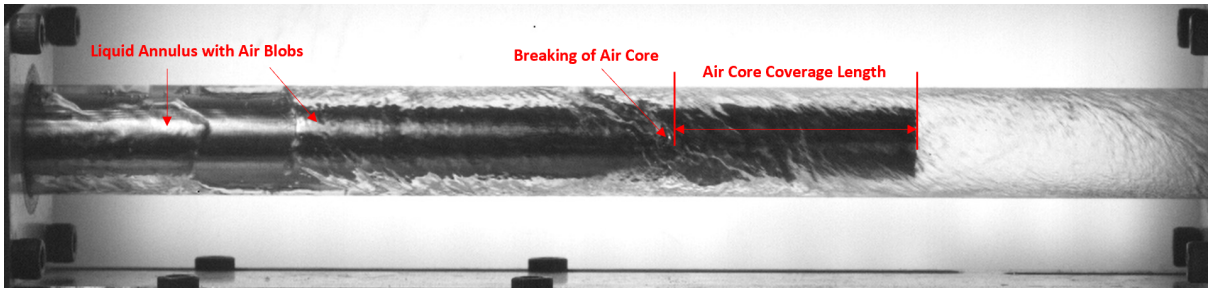

Figure 3.3: Photograph of Core Coverage Length for $\dot{V}_{water}$ = 1.5 GPM and $\dot{V}_{air}$ = 10 SCFM

As seen in the photograph, the core coverage length is the distance from the retrieval tube inlet to the point at which the air core becomes unstable and breaks apart. When the core breaks apart, some of the air from the air core is carried with the liquid annulus and exits with the liquid.

Figure 3.4 shows how core coverage length varies with superficial air velocity. In

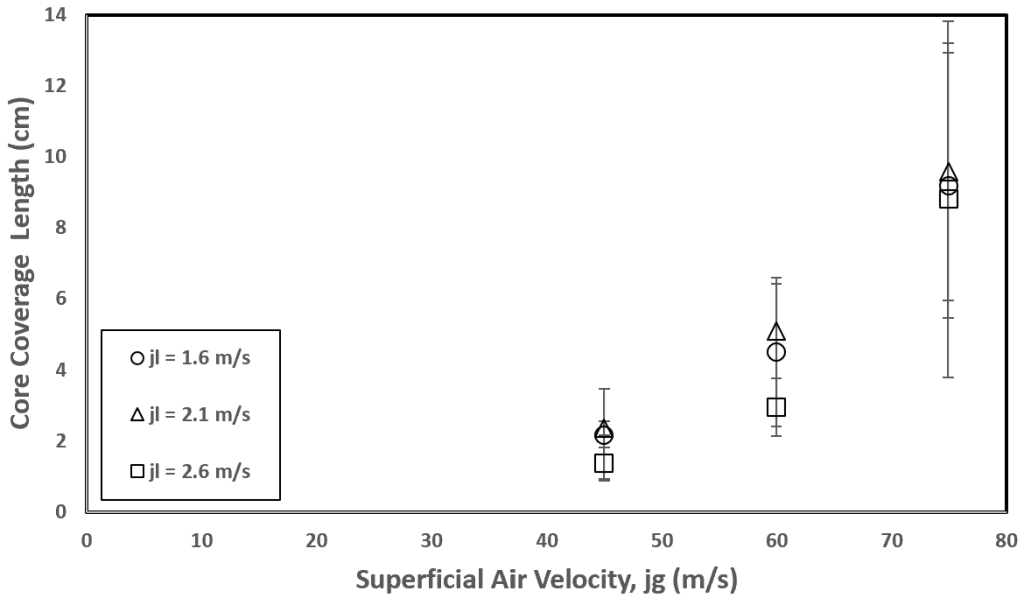

Figure 3.4: Core Coverage Length versus Superficial Air Velocity with retrieval tube positioned at 11.43 cm

the figure, average core coverage length is plotted with variability bars to represent the maximum and the minimum core coverage length for each case. The variability bars show the fluctuations in core coverage length for each case. Core coverage length is much more sensitive to the changes in air and water velocities compared to core diameter. Core coverage length tends to increase with increase in air velocity for a given water velocity. Higher velocity of air increases the tangential momentum of air allowing for a larger and longer air core. However, increases in water velocity slightly decrease core coverage length as shown in Figure 3.5. This is likely due to the increase in pressure drop through the liquid exit line causing more of the air from the air core to flow through the retrieval tube. Because more air is flowing through the retrieval tube, the distance at which the air core extends past the retrieval tube inlet decreases. In the case of increases in air velocity at a given water velocity, the increase in pressure drop through the retrieval tube creates more resistance for the air core. Therefore, the higher resistance causes the air core to travel further up the retrieval tube. It is important to note that as the air flowrate increases, the fluctuation in the core coverage length becomes larger. For cases where the superficial air velocity is 75 m/s, the air core covered well past the retrieval tube but the location at which the core collapsed changed frequently.

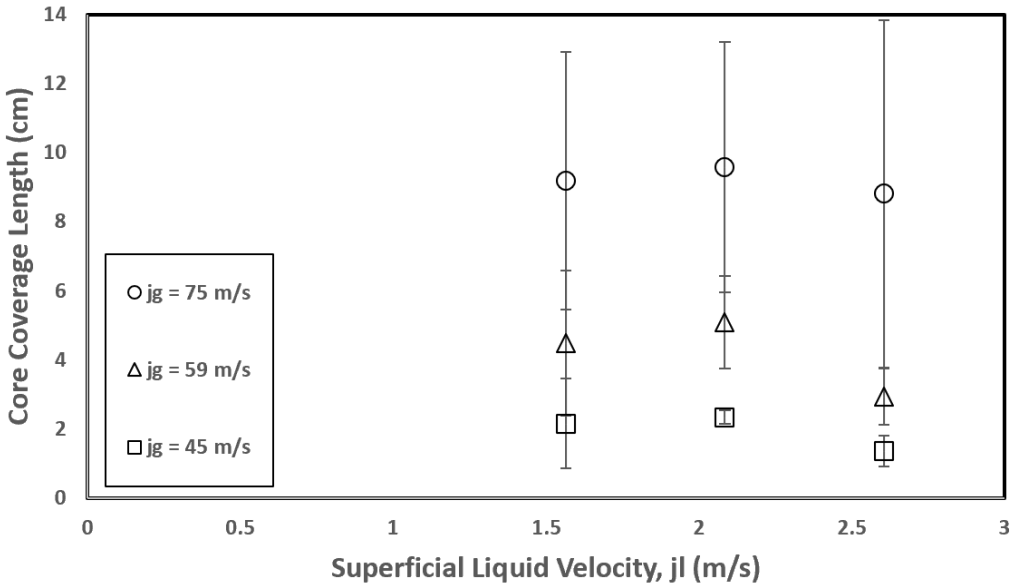

Figure 3.5: Air Core Coverage Length versus Superficial Liquid Velocity with retrieval tube positioned at 11.43 cm

3.3 Phase Separation Efficiency

The separation efficiency for each of the cases was recorded by measuring the mass of the entrained liquid that was collected through the retrieval tube. For calculating separation efficiency, it was assumed that all the air flowing through the injection tubes and injection passages was collected by the retrieval tube.

As seen in Figure 3.6, increases in air velocity increase separation efficiency at constant liquid velocity. This is likely due to the behavior in core coverage length and the effect of pressure drop through the retrieval tube and the liquid exit line. As air velocity is increased, more air flows through the retrieval tube and increases the pressure drop through the retrieval tube line. This added resistance in the retrieval tube line causes the air core to extend further past the retrieval tube inlet and in most cases, causes some of the air from the air core to get carried with the liquid annulus through the liquid exit. This prevents liquid in the annulus from getting entrained into the retrieval tube improving separation efficiency. When liquid velocity is increased, core coverage length slightly decreases as seen in Figure 3.5. Pressure drop through the liquid exit line increases and causes the liquid to enter the retrieval tube which has less resistance decreasing the separation efficiency. The amount of air leakage was assumed to be small

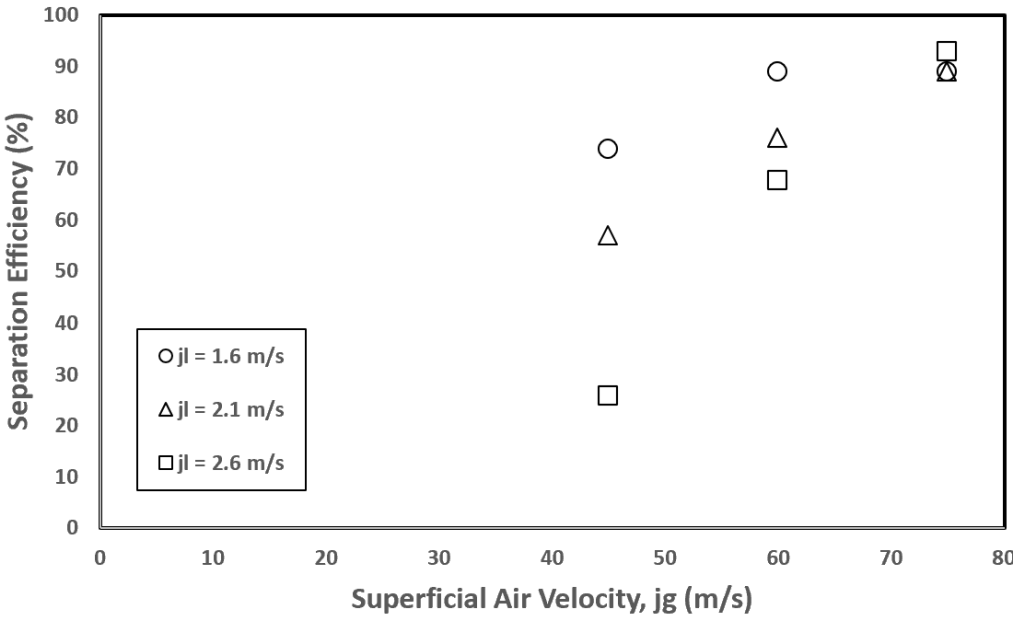

Figure 3.6: Separation Efficiency versus Superficial Air Velocity with retrieval tube positioned at 11.43 cm

and therefore, it was assumed that all of air is collected through the retrieval tube for calculating separation efficiency.

The effect of air core diameter on separation efficiency was determined to be not significant for the flowrates tested since the air core diameter was larger than the outer diameter of the retrieval tube for all cases. The changes in air core diameter were also small with changes in air and liquid velocities. However, the core coverage length varied significantly with air flowrate and is an important parameter for separation efficiency. The separation efficiency is plotted as a function of average core coverage length in Figure 3.7. For each superficial water velocity, the separation efficiency increases with increasing core coverage length and increasing superficial air velocity. For a given superficial water velocity, there is a minimum core coverage length needed for high separation efficiency. In order to achieve a separation efficiency close to 90%, the air core needed to extend over 8.5 cm past the inlet of the retrieval tube. This is important information when considering the optimal operating conditions for the system. If the core coverage length is not sufficiently long, there is possibility of re-entrainment of liquid droplets due to the air core collapsing near the retrieval tube inlet. For the given flowrate conditions, long core coverage length is critical for high separation efficiency.

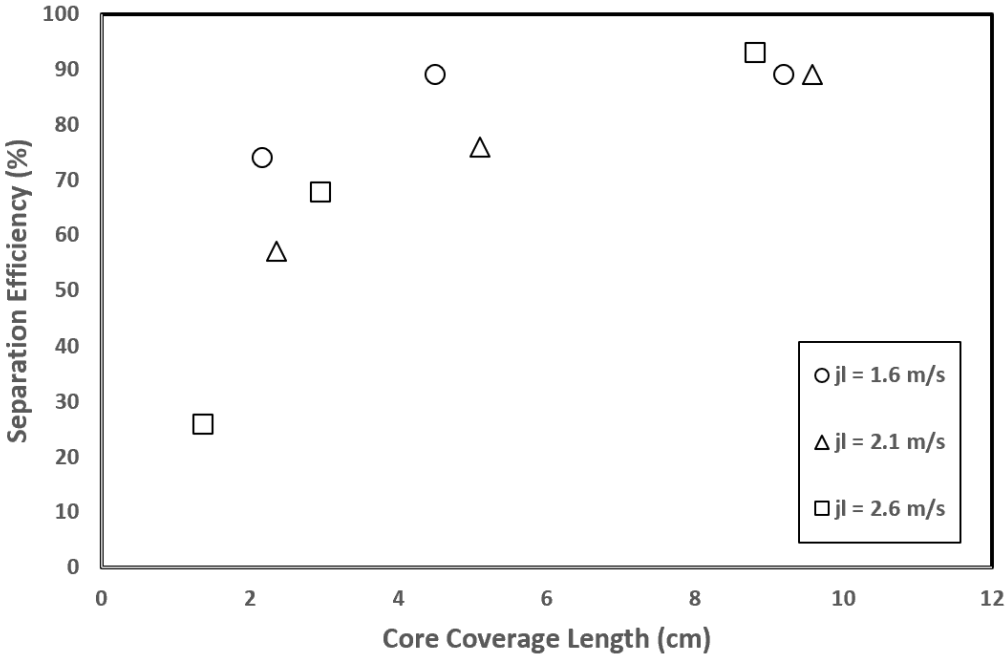

Figure 3.7: Average Core Coverage Length versus Separation Efficiency with retrieval tube positioned at 11.43 cm

3.4 Effect of Retrieval Tube Position on Core coverage Length and Separation Efficiency

The position of the retrieval tube with respect to the air core is an important parameter for the separation process. Having the air core envelop the retrieval tube inlet is critical for high separation efficiency. In the earlier experiments, the retrieval tube position was kept fixed at 11.43 cm away from the injection location. However, whether this position was optimal for separation was not well understood. For the same inlet conditions, the position of the retrieval tube could change the core coverage length. The effect of the retrieval tube position was studied by moving the retrieval tube farther away from the location of injection. For the same range of water and air flowrates, experiments were conducted for retrieval tube positions at 14.61 cm and 17.78 cm away from the point of injection. The data for core coverage length comparing the three retrieval tube positions is shown in Figure 3.8. For most of the cases, there is a general trend of a decrease in core coverage length as the retrieval tube inlet is positioned farther away from the injection location. This is likely due to the decrease in tangential momentum as the core travels through the separator tube. As the air core travels through the separator tube,

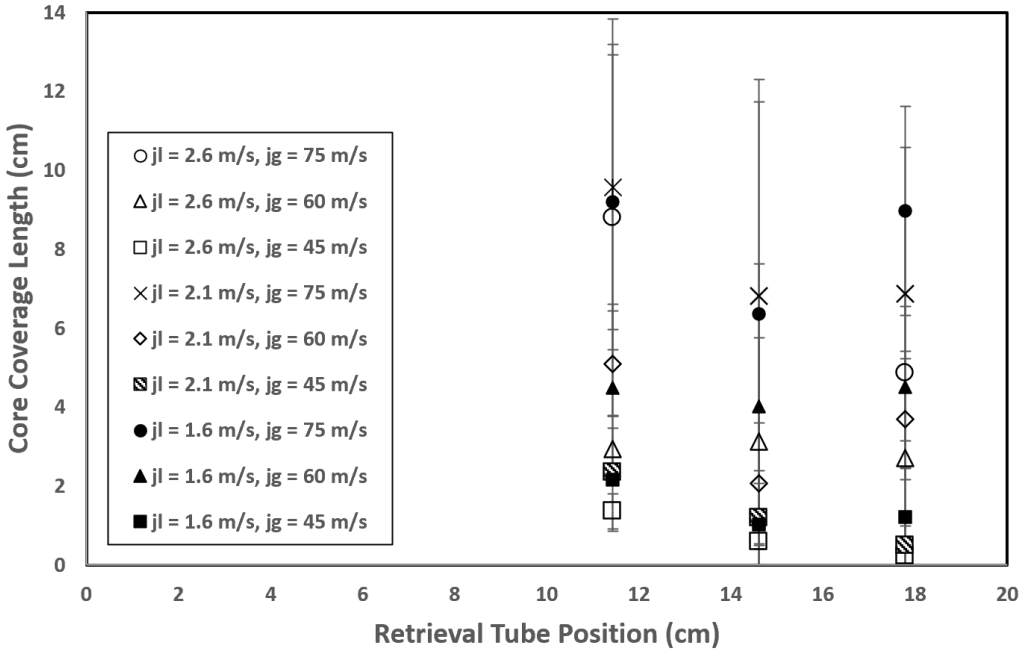

Figure 3.8: Core Coverage Length versus Retrieval Tube Position

more of the tangential momentum is converted into axial momentum or is dissipated and the air core becomes less stable. However, a nonlinear behavior is observed for higher water and air velocities. At higher flowrates, core coverage length fluctuates more as discussed earlier. The nonlinear behavior is likely attributed to the larger fluctuations and an increase in variability at higher flowrates.

The data for separation efficiency as retrieval tube position is varied is plotted in Figure 3.9. The separation efficiency behaves similar to that of core coverage length. For low water and air velocities, the separation efficiency decreases due to the air core collapsing closer to the retrieval tube inlet. When the air core collapses closer to the retrieval tube inlet, more liquid enters through the retrieval tube decreasing separation efficiency. For these cases, the highest separation efficiency was observed when the retrieval tube was positioned closest to the injection point. For higher water and air velocities, the nonlinear parabolic behavior is again observed. For the test section configuration, the position of the retrieval tube closest to the injection point achieved the best performance in separation.

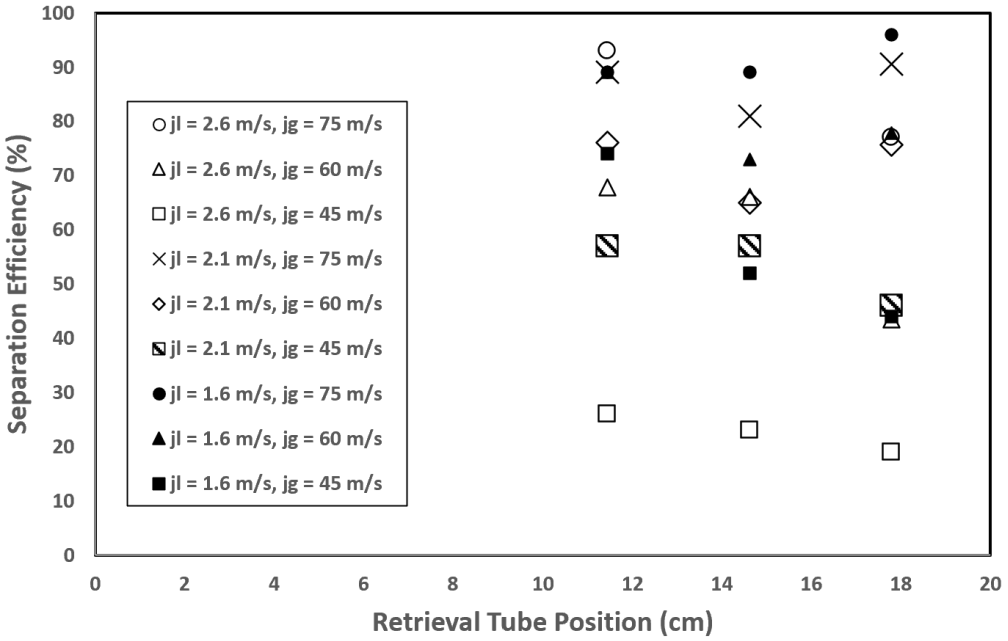

Figure 3.9: Separation Efficiency versus Retrieval Tube Position

3.5 Effect of Injector Diameter on Core Coverage Length and Separation Efficiency

The tangential velocity of both the liquid and air plays an important role for the formation of the air core and the separation efficiency. In the data for which is shown in Figure 3.1 to Figure 3.9, the diameter of the injection tubes and injection passages was fixed at 6.35 mm. Therefore, the tangential velocities of the liquid and air were varied through changes in the respective flowrates. A set of experiments was run by increasing the diameter of the injection tubes and injection passages to 9.53 mm. The same set of liquid and air flowrates was used except one additional air flowrate of 12 SCFM was added to the test cases. The retrieval tube position was fixed at 11.43 cm. Due to the larger injector diameter, the superficial liquid velocity ranged from 0.69 m/s to 1.15 m/s and the superficial air velocity ranged from 19.8 m/s to 39.6 m/s. The data for average core coverage length for both injector diameters is shown in Figure 3.10. The tangential velocity of both fluids plays a significant role in the core coverage length. Although the ratios between the liquid momentum to the air momentum between the two sets of experiments are the same since the range of flowrates is the same, the individual velocities are now lower due to the larger injector diameter and there is less tangential momentum for the air core to

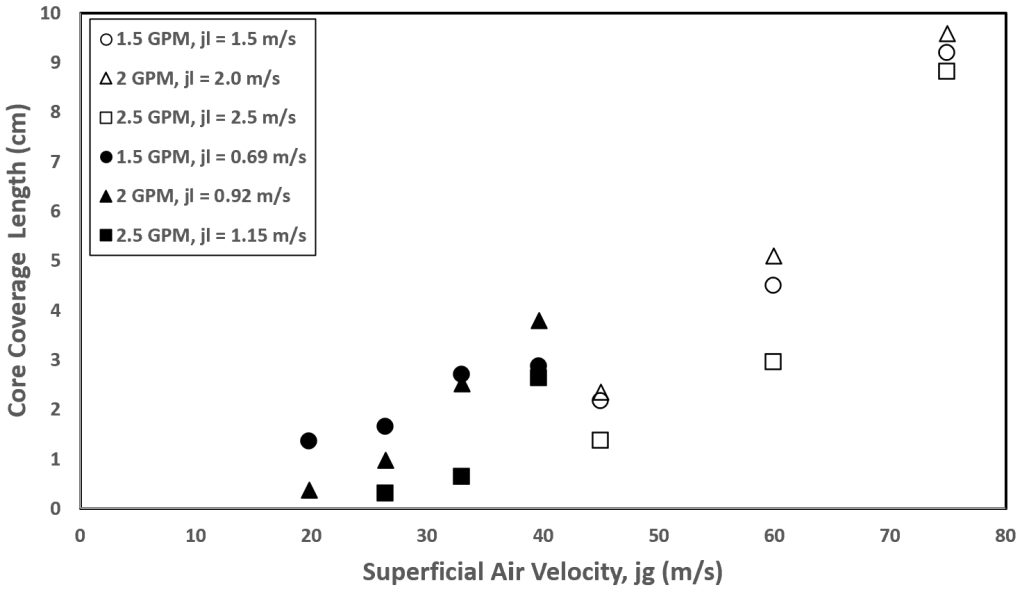

Figure 3.10: Average Core Coverage Length versus Superficial Air Velocity for Different Injector Diameters with retrieval tube positioned at 11.43 cm

form. Therefore, the core collapses closer to the retrieval tube inlet. The effect of this decrease in tangential velocity can also be observed for separation efficiency as shown in Figure 3.11. At 12 SCFM (jg = 39.6 m/s), the separation efficiency for the larger injector

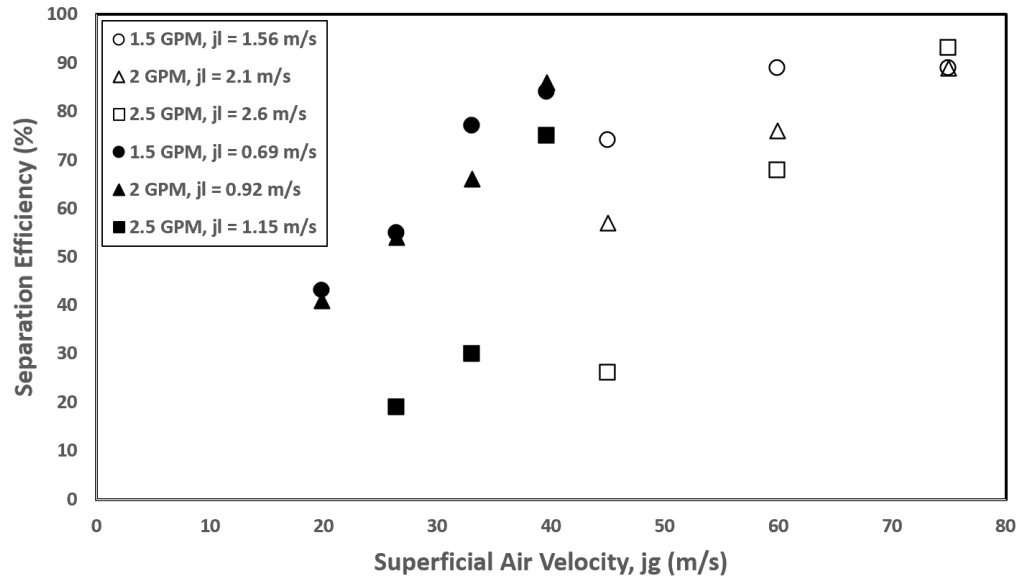

Figure 3.11: Separation Efficiency versus Superficial Air Velocity for Different Injector Diameters with retrieval tube positioned at 11.43 cm

diameter is only as high as 86% but is higher than that of the smaller injector diameter at similar j_g. This shows that tangential velocities of each fluid plays an important role for core coverage length and more importantly, the separation efficiency.

4 Conclusions

Adiabatic experiments simulating a single-stage dynamic flash evaporation and phase separation system were conducted.

1. In a swirl flow phase separator, superficial velocities of the liquid and air and position of retrieval tube were varied to study their effect on core diameter, air core coverage length, and separation efficiency and to point out optimal operating conditions for the system.

2. The core coverage length, position of the retrieval tube, and diameter of the injectors were determined to be important parameters for separation efficiency.

3. A sufficiently long core coverage length is needed to achieve high separation efficiency which is mainly influenced by superficial air velocity

4. For the range of flowrates and retrieval tube positions tested, the position of the retrieval tube closest to the injection point was determined to be most optimal.

5. Tangential velocity of liquid had a weak effect on core coverage length and separation efficiency and tangential velocity of air was found to be a more significant parameter of the system.

References

[1] Mohammad Ali Abdelkareem et al. “Recent progress in the use of renewable energy sources to power water desalination plants”. In: *Desalination* 435 (2018), pp. 97–113.

[2] Vasudevan Chandramouli, Jin Jen, and Vijay K Dhir. “Experimental Results for a Novel Flash Evaporation and Phase Separation System for Desalination of Sea Water”. In: *ASME Journal of Heat and Mass Transfer* 145.4 (2023), p. 041601.

[3] Hisham El-Dessouky et al. “Steady-state analysis of the multiple effect evaporation desalination process”. In: *Chemical Engineering & Technology: Industrial Chemistry-Plant Equipment-Process Engineering-Biotechnology* 21.5 (1998), pp. 437–451.

[4] Hisham T El-Dessouky, Hisham M Ettouney, and Yousef Al-Roumi. “Multi-stage flash desalination: present and future outlook”. In: *Chemical Engineering Journal* 73.2 (1999), pp. 173–190.

[5] Joyner Eke et al. “The global status of desalination: An assessment of current desalination technologies, plants and capacity”. In: *Desalination* 495 (2020), p. 114633.

[6] Z Guo and VK Dhir. “An Analytical and Experimental Study of a Swirling Bubbly Flow”. In: *National Heat Transfer Conference, HTD*. Vol. 112. 1989, pp. 93–100.

[7] Z Guo and VK Dhir. “Single-and two-phase heat transfer in tangential injection-induced swirl flow”. In: *International Journal of Heat and fluid flow* 10.3 (1989), pp. 203–210.

[8] Akili D Khawaji, Ibrahim K Kutubkhanah, and Jong-Mihn Wie. “Advances in seawater desalination technologies”. In: *Desalination* 221.1-3 (2008), pp. 47–69.

[9] Toufic Mezher et al. “Techno-economic assessment and environmental impacts of desalination technologies”. In: *Desalination* 266.1-3 (2011), pp. 263–273.

[10] Manjula Nair and Dinesh Kumar. "Water desalination and challenges: The Middle East perspective: a review". In: *Desalination and Water Treatment* 51.10-12 (2013), pp. 2030–2040.

[11] Haya Nassrullah et al. "Energy for desalination: A state-of-the-art review". In: *Desalination* 491 (2020), p. 114569.

[12] Sohum K Patel et al. "The relative insignificance of advanced materials in enhancing the energy efficiency of desalination technologies". In: *Energy & Environmental Science* 13.6 (2020), pp. 1694–1710.

[13] Mahmoud Shatat and Saffa B Riffat. "Water desalination technologies utilizing conventional and renewable energy sources". In: *International Journal of Low-Carbon Technologies* 9.1 (2014), pp. 1–19.

[14] Mohammad Abdul-Kareem Al-Sofi. "Fouling phenomena in multi stage flash (MSF) distillers". In: *Desalination* 126.1-3 (1999), pp. 61–76.

[15] Nicoleta Ungureanu, Valentin Vlăduț, and Gheorghe Voicu. "Water scarcity and wastewater reuse in crop irrigation". In: *Sustainability* 12.21 (2020), p. 9055.

[16] Vladimir Valentekovich, Daniel J Pafford, and Vijay K Dhir. "Theoretical and experimental investigation of swirl flow phase separators for microgravity applications". In: *New Mexico Univ, Transactions of the Fourth Symposium on Space Nuclear Power Systems p 347-350(SEE N 88-24254 17-73)*. 1987.

[17] Vladimir M Valentekovich and Vijay K Dhir. "Experimental investigation of a microgravity separator for two phase mixtures containing small volumes of gas/vapor". In: *Iˆˆ U SYSTEMS* 457 (1988).

[18] Domingo Zarzo and Daniel Prats. "Desalination and energy consumption. What can we expect in the near future?" In: *Desalination* 427 (2018), pp. 1–9.

[19] Jadwiga R Ziolkowska. "Is desalination affordable?—regional cost and price analysis". In: *Water Resources Management* 29 (2015), pp. 1385–1397.